Microwave Imaging Using Synthetic Radar Scheme Processing for the Detection of Breast Tumors

Abdullah K. Alqallaf [1], Rabie K. Dib [2], and Samir F. Mahmoud [1]

[1] Electrical Engineering Department, College of Engineering and Petroleum
Kuwait University, Kuwait
Al.qallaf@ku.edu.kw, samirfm2000@yahoo.com

[2] Electronics Engineering Department, College of Technological Studies
Public Authority of Applied Education and Training, Kuwait
rk.dib@paaet.edu.kw

Abstract ─ Microwave imaging of the human breast for detection of possible tumors is studied by applying the method of synthetic radar imaging using both simulation and theoretical results. The breast is modeled as a homogeneous medium having complex dielectric constant, while the tumor is modeled as a small spherical inhomogeneity. A flexible bow-tie antenna excited by a narrow-band pulse illuminates the breast and the reflected field is monitored as the antenna takes a number of discrete positions along the breast surface. The collected data is processed in a synthetic radar scheme to image the interior of the breast. Simulation results for tumor response are obtained and compared with theoretically obtained results. It is shown that a tumor of few millimeter radius, between 3 to 7 mm, can be detected and located with reasonable resolution. It is found that the tumor response increases with the tumor size at a given frequency band in an oscillatory fashion.

Index Terms ─ Breast, microwave imaging, synthetic radar, tumor detection.

I. INTRODUCTION

Microwave imaging of the breast has been of primary interest for few decades. The main purpose is the detection of possible tumors in their early stages. The tumor detection is based on the clear contrast between the complex dielectric constant of the normal breast tissue and the tumor [1-4]. Unlike the X-ray mammography, which is currently the main method of tumor detection, the microwave imaging method enjoys the property of being a nonionizing source of radiation which minimizes the cumulative side-effects to healthy breast tissues and consequently provides safer scanning alternative. In addition, the X-ray mammography has the basic limitation of small contrast between the diseased and normal tissues density, while the microwave imaging method scans in-depth penetration of the breast tissues by applying low power and longer wavelength signals to provide more accurate breast modal at the regular scanning conditions [5-8, 32]. There are mainly two approaches for microwave imaging. In the first approach, the breast is illuminated and the scattered field is used in an inverse scattering algorithm to construct an image of the electrical properties of the breast tissues. However, this inverse problem is considered an ill-conditioned nonlinear one and normally requires intensive computational work [9-11]. This is so due to the heterogeneous nature of the breast medium. However, some initial successful experimental results appear in [12-13]. The second approach is based on synthetic radar imaging that focus waves on small volume that is, in turn, scanned throughout the breast. This approach is also known as 'Confocal Microwave imaging'. This method has been investigated by Hagness and his group [14-17], and by Fear et al. [18-21] who confirm the method by simulation and experiment. A more recent study presents a tomographic based microwave system and signal processing to extract the tumor information from the background information and then to reconstruct the image through confocal method [31]. However, no attempt is made to study the resolution power of tumor location and the dependence of reflection level on tumor size.

In this paper, we introduce a parametric study of the resolution power of the confocal microwave imaging method. We intend to test the effectiveness of the synthetic radar approach for locating tumors using simple antenna driven by narrow band pulse. We also present results on the dependence of the reflection level on the tumor size. Both analytical and simulation results are obtained for assumed tumors of different size and location. We do so by modeling the breast and the illuminating antenna as illustrated in Section 2. Simulation results that include the resolution of tumor detection and the dependence of the reflected signal on

Submitted On: March 13, 2015
Accepted On: February 20, 2016

the tumor size are demonstrated in Section 3. In Section 4, analytical derivation of the response of a spherical tumor is presented. The theoretical results are compared with those obtained by simulations and are followed by concluding remarks.

II. THE BREST MODEL AND THE ANTENNA

Two possible positions for the breast can be used during imaging: the supine position and the prone position. In the supine position the breast is oriented upwards and flattened out, while in the prone position the breast is oriented downwards [17]. Further, it is found that the supine position is more practical for measuring process. Therefore, in this paper, we focus our study in the paper on the supine position. The breast is then modeled as a rectangular box with upper surface coinciding with $Z = 0$ plane as shown in Fig. 1. The width of the breast is taken equal to 20 cm, and the sides are loaded with matched loads. The depth is assumed equal to 15 cm. The breast medium is assumed homogeneous with conductivity σ (S/m) and relative permittivity ε_r. A possible tumor of spherical shape with radius 'a' exists at a depth d, i.e., at $Z = -d$. The tumor has a contrasting conductivity σ_s and relative permittivity ε_{rs}. An antenna is placed with its phase center at the origin of (x,y,z) coordinate system and radiates in the breast medium. The planar antenna lies directly on the breast. A suitable thin layer is placed between the breast surface and the antenna. The material of the layer should electrically match the body so that no reflection occurs at the surface [17]. The center of the spherical tumor lies at ($X = -L$ and $Z = -d$) as shown in Fig. 1. A rotated Cartesian coordinates (x,y,z) has origin at the sphere center. While the relative permittivity ε_r of normal tissues is around 10, that of the tumor is around 50. There is also contrast between the conductivities, being about 0.15 S/m for normal tissue and 0.7 S/m for tumors [17]. The choice of a suitable antenna for breast cancer detection is very crucial matter. The antenna is required to be compact, wide band, low profile, light weight, and flexible enough to be placed directly on the breast.

Recently, several antenna designs for breast cancer detection have been proposed including the dielectric resonator antenna [22-23], the stacked patch antenna [24], the wide slot UWB antenna [25], and the flexible bow-tie [26, 30]. All of these antennas meet the required traits of a breast cancer sensor. We have selected the flexible bow-tie antenna for our investigation since it has the smallest size and it is mechanically flexible to have a good contact with the breast. The antenna geometry and dimensions are chosen as in Fig. 2 and Table 1 to operate around the center frequency of 6 GHz. This frequency is chosen as a compromise between required depth of penetration in the tissues and the tumor location with acceptable resolution. The metal body of the bow-tie is printed on two thin flexible dielectric sheets as suggested in [26, 29] and is fed by a microstrip line as shown in Fig. 2. The total thickness of the two dielectric sheets equals 0.1287 mm. The dielectric sheet is 0.05 mm thick and has a relative permittivity of 4. A matching scheme is designed with the feed line as shown in Fig. 2. The resulting reflection loss $|S_{11}|$, when the antenna is placed on a medium that resembles the breast electrical properties is given in Fig. 3. It is seen that a -10 dB reflection loss or more is secured in the frequency ranges 4.75-6.7 GHz.

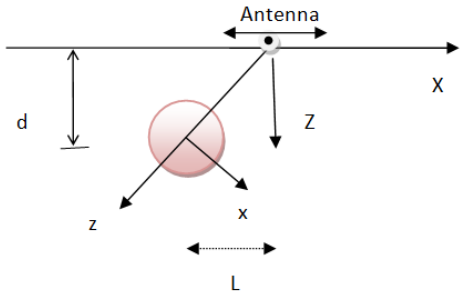

Fig. 1. Model of a spherical tumor of radius 'a' at depth d below the breast upper surface. The antenna lies on the surface at a lateral distance L from the tumor center.

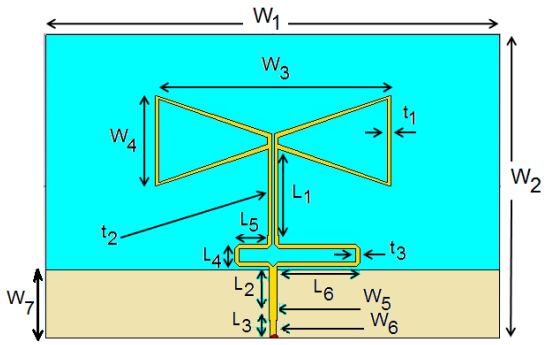

Fig. 2. Bow-tie antenna used for imaging. The antenna dimensions are given in Table 1. The antenna is placed on a medium with the breast-like permittivity.

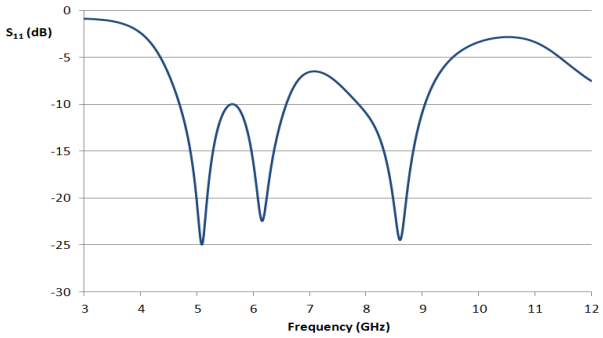

Fig. 3. The reflection $|S_{11}|$, in dB, versus the frequency, in GHz, where the antenna is placed on a medium with the breast-like permittivity.

Table 1: Bow-tie antenna dimensions used for imaging

Parameters	Length in (mm)
W_1	36
W_2	23.2
W_3	18.72
W_4	6.96
W_5	0.65
W_6	0.51
W_7	7.2
L_1	6.12
L_2	4.03
L_3	2.48
L_4	1.53
L_5	2.57
L_6	5.74
t_1	0.23
t_2	0.24
t_3	0.34

III. SIMULATION RESULTS

The antenna is placed on the breast surface and is fed by a pulse that covers a bandwidth of 500 MHz around 6 GHz center frequency. The pulse shape in the time domain is shown in Fig. 4. The pulse bandwidth is less than 10% of the center frequency. Within this narrow bandwidth, the breast electrical parameters can be assumed constants and therefore, one can accurately compensate for the propagation effects in the breast. One can apply the pulse at different discrete center frequencies to obtain multi-frequency images for the tumor.

The voltage waveform picked up by the antenna is monitored for, say, *M* different positions of the antenna as it is displaced along the *X*-axis. To remove the primary pulse and possible reflections from the skin layer of the breast, the average received waveform from the *M* positions is subtracted from each of the received waveforms. The resulting signals represent the scattered field from the tumor inhomogeneity at the *M* antenna positions. The next step is to process the *M* signals so as to synthetically focus the field at an arbitrary point within the breast. This leads to imaging the breast medium. In processing the *M* waveforms, we have to account for the variations of the antenna radiation pattern at the scanned points.

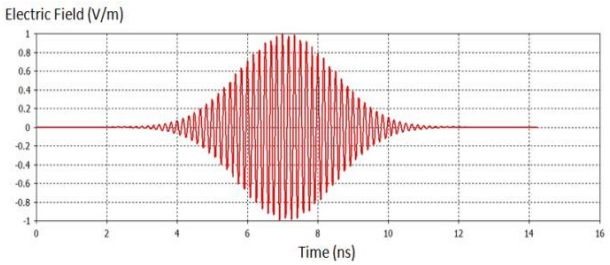

Fig. 4. The feeding pulse shape in the time domain.

The response obtained from a spherical tumor of radius 4 mm in the *X*-*Z* plane is shown is Fig. 5. The tumor is placed at $X = 0$ and $Z = -d = -30$ mm.

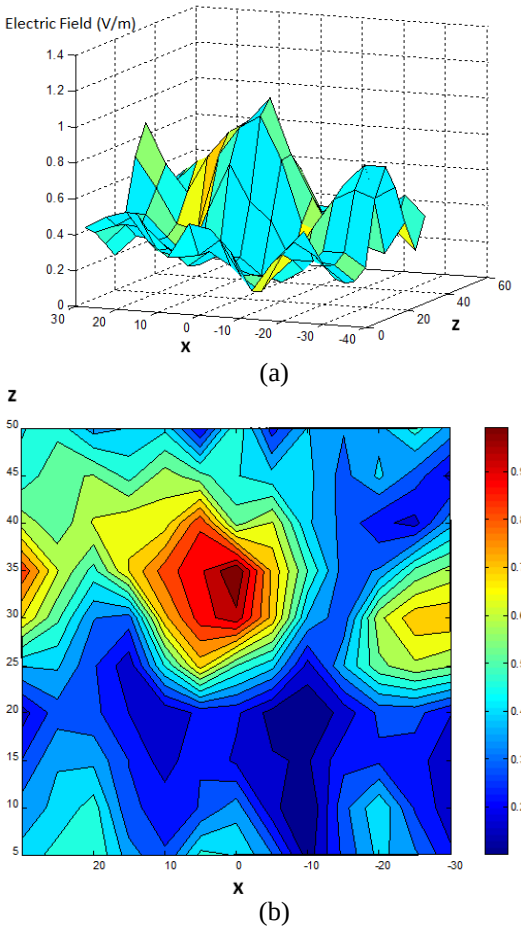

Fig. 5. Reflection response versus observing point on the x-z plane for 4 mm radius tumor: (a) 3-dimensional plot, and (b) contours of constant reflection.

The breast is modeled as a block of width 200 mm, and depth of 100 mm. The response in Fig. 5 (a) is obtained for $M = 17$ positions of the antenna on the $Z = 0$ plane with spacing of 8 mm between positions. The contours of constant response levels are shown in Fig. 5 (b). Figures 6 (a), (b) show the same response as in Fig. 5 (a), (b), except that the tumor radius is increased to 6 mm. It is clear from both figures that there is a clear peak response at the exact position and depth of the tumor. The resolution may be determined by the region where the response is reduced to 50% of the peak value. For the 4 mm tumor, the resolution region covers 20 mm about the *X* position and about 15 mm in the *Z*-direction. This means that two tumors separated horizontally by less than 20 mm or vertically by 15 mm cannot be distinguished and will show as one tumor. It is interesting to study the reflection level as a function of

the tumor radius at a given depth. The normalized reflection response for different tumor sizes at 6 GHz center frequency is presented for d = 30 mm in Fig. 7. It is seen that the response increases with tumor size in an oscillatory fashion. There is a minimum response for tumor radii of 3 mm and 5 mm. These minima will move to other values of tumor radii if the center frequency changes.

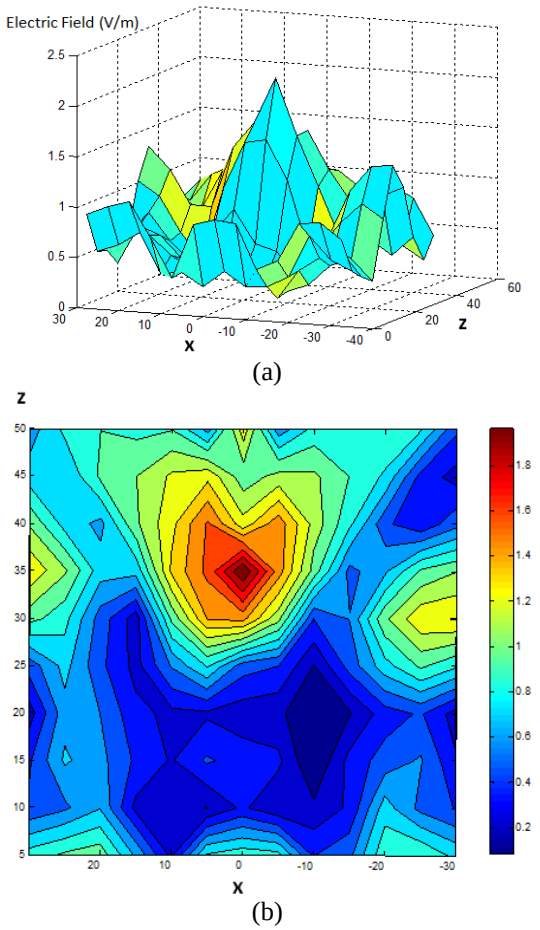

Fig. 6. Reflection response versus observing point on the x-z plane for 6 mm radius tumor: (a) 3-dimensional plot, and (b) contours of constant reflection.

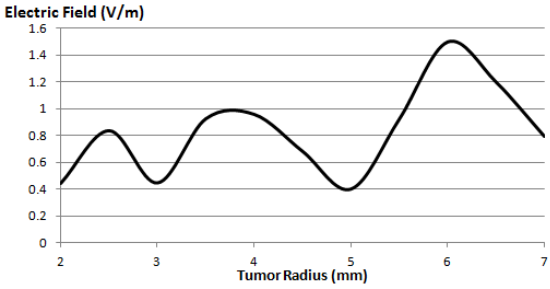

Fig. 7. Simulated reflection response vs. tumor radius (mm) at 6 GHz.

IV. THEORETICAL ANALYSIS

In this section we derive the scattered field from the tumor inhomogeneity. The antenna illuminates the tumor by an incident wave which is generally a spectrum of plane waves. However, we can assume that in the vicinity of the tumor whose dimensions are less than the applied wavelength, the incident wave is a single plane wave directed from the antenna phase center to the tumor center (in the z-direction). Adopting this assumption, we write the incident E and H field as:

$$E_x^i = E_o e^{-jkz} = E_o e^{-jkr\cos\theta}, \quad (1)$$

$$H_y^i = \frac{E_o}{\eta} e^{-jkr\cos\theta}, \quad (2)$$

where a time harmonic field dependence as $exp(j\omega t)$ has been assumed with $j = \sqrt{-1}$ and the complex wave number $k = \omega\sqrt{\mu_0\epsilon_0(\epsilon_r - \frac{j\sigma}{\omega\epsilon_0})}$. The radial coordinate r is measured from the sphere center, and η is the wave impedance in the breast medium. It is useful to obtain the radial fields in order to pursue the analysis to obtain the scattered fields in the spherical coordinate system (r,θ,ϕ). In terms of the spherical wave functions, the incident radial E takes the form:

$$E_r^i = \frac{E_o\cos\phi}{jkr}\sum j^{-n}(2n+1)\hat{J}_n(kr)\frac{\partial}{\partial\theta}P_n^{(1)}(\cos\theta)), \quad (3)$$

here $\hat{j}_n\,(kr)$ is the spherical Bessel function as defined in [28], and $P_n^{(1)}(\cos\,\theta)$ is the associated Legendre polynomial [27]. The radial E in (4) is also derivable from a magnetic vector potential A_r, so that,

$$E_r^i = (j\omega\epsilon)^{-1}\left[\frac{\partial^2}{\partial r^2} + k^2\right]A_r^i = (j\omega\epsilon)^{-1}\,\frac{n(n+1)}{r^2}\,A_r^i.$$

Therefore:

$$A_r^i = \frac{E_o}{\omega\mu}\cos\phi\sum_{n=0}^{\infty}a_n J_n(kr)P_n^{(1)}(\cos\theta), \quad (4)$$

where $a_n = j^{-n}(2n+1)/(n(n+1))$. Treating the radial magnetic field in the same way, we arrive at the incident electric vector potential F_r as [28]:

$$F_r^i = \frac{E_o}{k}\sin\phi\sum_{n=0}^{\infty}a_n J_n(kr)P_n^{(1)}(\cos\theta). \quad (5)$$

The scattered fields have similar form except that $\hat{j}_n(kr)$ is replaced by the spherical Hankel function $\hat{H}_n(kr)$. The total external field to the sphere (incident + scattered) is given by:

$$A_r^{ex} = \frac{E_o}{\omega\mu}\cos\phi\sum_{n=0}^{\infty}(a_n J_n(kr) + b_n\hat{H}_n(kr)P_n^{(1)}(\cos\theta)$$
$$F_r^{ex} = \frac{E_o}{k}\sin\phi\sum_{n=0}^{\infty}(a_n J_n(kr) + c_n\hat{H}_n(kr)P_n^{(1)}(\cos\theta) \quad (6)$$

where b_n and c_n coefficients are, so far, unknown to be determined from the boundary conditions at the spherical

surface. The next step towards the determination of the fields everywhere is to write down the internal fields inside the spherical tumor, namely:

$$A_r^{in} = \frac{E_o}{\omega\mu}\cos\phi\sum_{n=1}^{\infty} d_n J_n(k_s r)P_n^{(1)}(\cos\theta)$$
$$F_r^{ex} = \frac{E_o}{k_s}\sin\phi\sum_{n=1}^{\infty} e_n J_n(k_s r)P_n^{(1)}(\cos\theta) \quad , \quad (7)$$

where again d_n and e_n are unknown coefficients. Note that k_s is the wave number in the spherical tumor. Namely, $k_s = \omega\sqrt{\mu_0\epsilon_0(\epsilon_{rs} - \frac{j\sigma_s}{\omega\epsilon_0})}$.

Now, we are ready to apply the boundary conditions requiring the continuity of the $\theta$and ϕ–field components at the spherical surface. This leads to the determination of the scattered field coefficients b_n and c_n as given in the Appendix.

The scattered E_θ component in the external region is given by:

$$E_\theta^S(r,\theta) = \frac{-E_o}{kr}cos\emptyset\begin{bmatrix}\sum_{n=1}^{N} c_n\widehat{H}_n(kr)\frac{P_n'(cos\theta)}{sin\theta} \\ +jb_n\widehat{H}_n'(kr)\frac{\partial P_n'(cos\theta)}{\partial\theta}\end{bmatrix}. \quad (8)$$

The summation term is truncated after N terms, where N depends on the tumor size. Numerical calculations show that N = 5 gives acceptable convergence up to tumor radius of 7 mm at 6 GHz applied frequency. The scattered field at the transmitting antenna is equal to: $E_\theta(r_1,\pi)\,(-\frac{d}{r_1})$, where $r_1 = \sqrt{d^2 + L^2}$ and we have assumed that the antenna major polarization is along X' direction.

Next, signal processing is applied to realize focusing on the tumor for M positions of the antenna at $L = i\Delta$; i=0, 1, 2 … (M -1). The net signal for the M positions of the antenna is:

$$E_{total} = \sum_{i=0}^{M-1}\,[E_\theta(r_1,\pi)\,(-\tfrac{d}{r_1})]\,\exp[+2jkr_1]. \quad (9)$$

As an example we plot (11) versus the tumor radius 'a' in mm for an applied frequency of 6 GHz, and depth d = 30 mm in Fig. 8. The antenna is positioned in 17 equidistant positions with spacing Δ = 10 mm. The field is normalized relative to the incident E. It is noted that the response tends to increase with the tumor radius, but in an oscillatory manner. The theoretical result is compared with simulation in the same figure, and it is seen that there is a reasonable agreement. We have to bear in mind that the theoretical curve is computed for a single applied frequency (6 GHz), while the simulation curve is done for a band of frequency (5.75 – 6.25 GHz). In order to study the effect of varying the applied frequency, the tumor response is plotted versus the frequency between 5-7.5 GHz at three different tumor radii in Fig. 9. It is seen that depending on the tumor radius, there is an optimum frequency for tumor detection. For example a tumor of 3 mm radius is not detectable at f~6.1 GHz while it is well detected at f~7.0 GHz. On the other hand, the optimum frequency for detecting a tumor of 6 mm radius is f~6.2 GHz. We thus conclude the importance of imaging the breast by several narrow band pulses of distinct center frequencies.

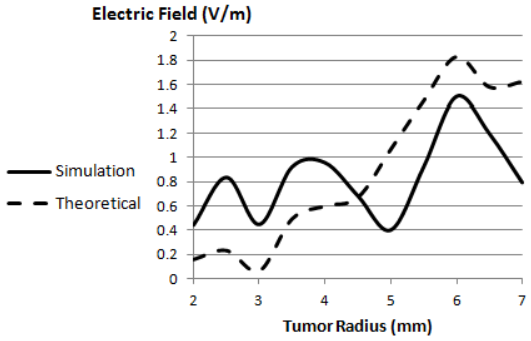

Fig. 8. Simulation and theoretical normalized reflection response vs. tumor radius (mm) at 6 GHz.

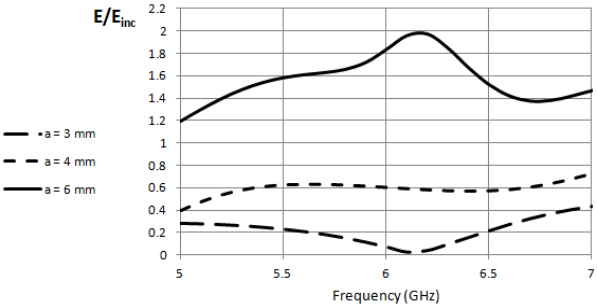

Fig. 9. Theoretical reflection response for three different tumor radii a = 3, 4, and 6 mm vs. center.

V. CONCLUSION

In this paper we have presented a study of microwave imaging of the human breast for possible tumor detection by applying the method of synthetic radar imaging. Both analytical and simulation results are presented for assumed tumors of different size and location. The breast is modeled as a homogeneous medium having complex dielectric constant, while the tumor is modeled as a small spherical inhomogeneity. The breast is illuminated by a microwave pulse of narrow bandwidth through a bow-tie antenna and the reflected field is monitored as the antenna is positioned at a number of discrete positions along the breast surface. Signal processing is applied to the collected data to focus the wave at different points to scan the whole breast. It has been demonstrated that a spherical tumor of few millimeter radius can be detected with reasonable resolution using a pulse of 6 GHz center frequency and 0.5 GHz bandwidth. The response of a tumor generally increases with its size, but in an oscillatory manner. The simulation results are supported by analytical results

where a reasonably good agreement is observed. Our study also shows that the optimum frequencies for detecting tumors depend on the tumors' radii. Finally, it is recommended that images should be taken at few distinct frequencies in the range 5-7 GHz in order to detect tumors of different sizes.

VI. APPENDIX

The coefficients b_n and c_n in (8) are obtained from the boundary conditions at the spherical surface $r=a$ as:

$$b_n / a_n = [\bar{\eta}_s R_{ns} J_n(ka) - J_n^{'}(ka)] / [\hat{H}_n^{'}(ka) - \bar{\eta}_s R_{ns} \hat{H}(ka)], \quad \text{(A1)}$$

$$c_n / a_n = [\bar{k}_s R_{ns} \hat{J}_n(ka) - \hat{J}_n^{'}(ka)] / [\hat{H}^{'}(ka) - \bar{k}_s R_{ns} \hat{H}(ka)], \quad \text{(A2)}$$

where the dash on the Bessel and Hankel spherical functions denotes differentiation with respect to the argument,

$$\bar{\eta}_s = \eta_s/\eta, \ \overline{k_s} = \frac{k_s}{k}, \text{ and } R_{ns} = \hat{J}_n^{'}(k_s a)/\hat{H}_n^{'}(k_s a).$$

ACKNOWLEDGMENT

This work was supported by Kuwait University Research Grant No. [RE02/12].

REFERENCES

[1] A. J. Surowiec, S. S. Stuchly, J. R. Barr, and A. Swarup, "Dielectric properties of breast carcinoma and the surrounding tissues," *IEEE Trans. Biomed. Eng.*, vol. BME-35, pp. 257-263, Apr. 1988.

[2] W. T. Joines, Y. Zhang, C. Li, and R. L. Jirtle, "The measured electrical properties of normal and malignant human tissues from 50 to 900 MHz," *Med. Phys.*, vol. 21, pp. 547-550, Apr. 1994.

[3] S. S. Chaudhary, R. K. Mishra, A. Swarup, and J. M. Thomas, "Dielectric properties of normal and malignant human breast tissues at radiowave and microwave frequencies," *Indian J. Biochem. Biophys.*, vol. 21, pp. 76-79, Feb. 1984.

[4] S. C. Hagness, K. M. Leininger, J. H. Booske, and M. Okoniewski, "Dielectric characterization of human breast tissue at microwave frequencies," *Presented at the 2nd World Congr. Microwave and Radio Frequency Processing*, Orlando, FL, Apr. 2000.

[5] M. Brown, F. Houn, E. Sickles, and L. Kessler, "Screening mammography in community practice," *Amer. J. Roentgen.*, vol. 165, pp. 1373-1377, Dec. 1995.

[6] P. T. Huynh, A. M. Jarolimek, and S. Daye, "The false-negative mammogram," *Radiograph.*, vol. 18, no. 5, pp. 1137-1154, 1998.

[7] J. G. Elmore, M. B. Barton, V. M. Moceri, S. Polk, P. J. Arena, and S. W. Fletcher, "Ten-year risk of false positive screening mammograms and clinical breast examinations," *New Eng. J. Med.*, vol. 338, no. 16, pp. 1089-1096, 1998.

[8] V. P. Jackson, R. E. Hendrick, S. A. Feig, and D. B. Kopans, "Imaging of the radiographically dense breast," *Radiology*, vol. 188, pp. 297-301, Aug. 1993.

[9] S. Caorsi, G. L. Gragnani, and M. P. Pastorino, "Reconstruction of dielectric permittivity distributions in arbitrary 2-D inhomogeneous biological bodies by a multiview microwave numerical method," *IEEE Trans. Med. Imag.*, vol. 12, pp. 232-239, June 1993.

[10] A. E. Souvorov, A. E. Bulyshev, S. Y. Semenov, R. H. Svenson, A. G. Nazarov, Y. E. Sizov, and G. P. Tatsis, "Microwave tomography: a two-dimensional Newton iterative scheme," *IEEE Trans. Microwave Theory Tech.*, vol. 46, pp. 1654-1659, Nov. 1998.

[11] M. Bertero, M. Miyakawa, P. Boccacci, F. Conte, K. Orikasa, and M. Furutani, "Image restoration in chirp-pulse microwave CT (CP-MCT)," *IEEE Trans. Biomed. Eng.*, vol. 47, pp. 690-699, May 2000.

[12] P. M. Meaney, K. D. Paulsen, J. T. Chang, M. W. Fanning, and A. Hartov, "Nonactive antenna compensation for fixed-array microwave imaging–Part II: imaging results," *IEEE Trans. Med. Imag.*, vol. 18, pp. 508-518, June 1999.

[13] P. M. Meaney, M. W. Fanning, D. Li, S. P. Poplack, and K. D. Paulsen, "A clinical prototype for active microwave imaging of the breast," *IEEE Trans. Microwave Theory Tech.*, vol. 48, pp. 1841-1853, Nov. 2000.

[14] S. C. Hagness, A. Taflove, and J. E. Bridges, "Two-dimensional FDTD analysis of a pulsed microwave confocal system for breast cancer detection: fixed-focus and antenna-array sensors," *IEEE Trans. Biomed. Eng.*, vol. 45, pp. 1470-1479, Dec. 1998.

[15] S. C. Hagness, A. Taflove, and J. E. Bridges, "Wideband ultra low reverberation antenna for biological sensing," *Electron. Lett.*, vol. 33, no. 19, pp. 1594-1595, 1997.

[16] S. C. Hagness, A. Taflove, and J. E. Bridges, "Three-dimensional FDTD analysis of a pulsed microwave confocal system for breast cancer detection: design of an antenna-array element," *IEEE Trans. Antennas Propagat.*, vol. 47, pp. 783-791, May 1999.

[17] X. Li and S. C. Hagness, "A confocal microwave imaging algorithm for breast cancer detection," *IEEE Microwave Wireless Comp. Lett.*, vol. 11, pp. 130-132, Mar. 2001.

[18] E. Fear and M. Stuchly, "Microwave system for breast tumor detection," *IEEE Microwave Guided Wave Lett.*, vol. 9, pp. 470-472, Nov. 1999.

[19] E. C. Fear and M. A. Stuchly, "Microwave detection of breast cancer," *IEEE Trans. Microwave Theory Tech.*, vol. 48, pp. 1854-1863, Nov. 2000.
[20] E. C. Fear and M. A. Stuchly, "Microwave detection of breast tumors: comparison of skin subtraction algorithms," *Proc. SPIE*, vol. 4129, pp. 207-217, 2000.
[21] E. C. Fear, X. Li, S. C. Hagness, and M. A. Stuchly, "Confocal microwave imaging for breast cancer detection: localization of tumors in three dimensions," *IEEE Transactions on Biomedical Engineering*, vol. 49, no. 8, Aug. 2002.
[22] W. Huang and A. A. Kishk, "Compact wideband multi-layer cylindrical dielectric resonator antennas," *IEE Proc. Microw. Antennas Propag.*, vol. 1, no. 4, pp. 998-1005, 2007.
[23] W. Huang and A. A. Kishk, "Compact dielectric resonator antenna for microwave breast cancer detection," *IET Microwave, Antennas & Propagation*, vol. 3, iss. 4, pp. 638-644, 2009.
[24] R. Nilavalan, I. J. Craddock, A. Preece, J. Leendertz, and R. Benjamin, "Wideband microstrip patch antenna design for breast cancer detection," *IET Microw. Propag.*, vol. 1, no. 2, pp. 277-281, 2007.
[25] D. Gibbins, M. Klemm, I. J. Craddock, J. A. Leendertz, A. Preece, and R. Benjamin, "A comparison of a wide-slot and a stacked patch antenna for the purpose of breast cancer detection," *IEEE Transactions on Antennas and Propagation*, vol. 58, no. 3, pp. 665-674, 2010.
[26] A. C. Durgun, C. A. Balanis, C. R. Birtcher, and D. A. Allee, "Design, simulation, fabrication and testing of flexible bow-tie antennas," *IEEE Trans. on Antennas and Propagat.*, vol. 59, no. 12, 2011.
[27] M. Abramowitz and I. A. Stegun, ed., *Handbook of Mathematical Functions*, Chapter 10 by H. Antosiewice, Dover Publications, Inc., New York, 1970.
[28] R. F. Harrington, *Time Harmonic Electromagnetic Fields*, Chapter 6, McGraw Hill, 1961.
[29] A. A. Eldek, A. Z. Elsherbeni, and C. E. Smith, "Wideband modified printed bow-tie antenna with single and dual polarization for C and X-band applications," *IEEE Transaction on Antennas and Propagations*, vol. 53, no. 9, pp. 3067-3072, Sep. 2005.
[30] E. Porter, G. Walls, Y. Zhou, M. Popovic, and J. D. Schwartz, "A flexible broadband antenna and transmission line network for a wearable microwave breast cancer detection system," *Progress In Electromagnetics Research Letters*, vol. 49, pp. 111-118, Oct. 2014.
[31] Z. Wang, E. G. Lim, Y. Tang, and M. Leach, "Medical applications of microwave imaging," *The Scientific World Journal*, vol. 2014, 2014.
[32] P. K. Singh, S. K. Tripathi, R. Sharma, and A. Kumar, "Design & simulation of microstrip antenna for cancer diagnosis," *International Journal of Scientific & Engineering Research*, vol. 4, iss. 11, pp. 1821-1824, Nov. 2013.

Abdullah K. Alqallaf is an Assistant Professor with the Department of Electrical Engineering at the Kuwait University. He received the B.S. and M.S. degrees in Electrical Engineering from Kuwait University in 1996 and 1999, respectively, and the Ph.D. degree in Electrical Engineering from the University of Minnesota – Twin Cities, St. Paul, MN, in 2009. Alqallaf's research interests are Microwave Imaging Techniques, Multimedia Signal Processing, Communication, Bioinformatics and Medical Image Analysis. Alqallaf is an IEEE Board Member - Professional Activities - Kuwait section.

Rabie K. Dib is an Instructor with the Electronics Engineering Dept., College of Technological Studies at Public Authority of Applied Education and Training, Kuwait. He received the B.S. and M.S. degrees in Electrical Engineering from Kuwait University in 1999 and 2002, respectively. Dib's research interests are Electromagnetics, Communication, Antenna Design, Microwave Imaging Techniques and Analysis.

Samir F. Mahmoud is a Professor with the Department of Electrical Engineering at the Kuwait University. He received the B.S. in Electrical Engineering from the Electronic Engineering Dept., Cairo University, Egypt in 1964. He received the M.Sc. and Ph.D. degrees in the Electrical Engineering Department, Queen's University, Kingston, Ontario, Canada in 1970 and 1973, respectively. He was a Visiting Research Fellow at the Cooperative Institute for Research in Environmental Sciences (CIRES), Boulder, CO, doing research on Communication in Tunnels during the academic year 1973-1974. He spent two sabbatical years, 1980-1982, between Queen Mary College, London and the British Aerospace, Stevenage, where he was involved in design of antennas for satellite communication. Recently, he has visited several places including Interuniversity Micro-Electronics

Centre (IMEC), Leuven, Belgium and spent a sabbatical leave at Queen's University and the Royal Military College, Kingston, Ontario, Canada in 2001-2002. His research activities have been in the areas of antennas, geophysics, tunnel communication, and e.m wave interaction with composite materials. Mahmoud is a Fellow of IET and one of the recipients of the best IEEE/MTT paper for 2003.